

## Electronic Raman spectra of shallow acceptors in semi-insulating GaAs

K. Wan and Ralph Bray

*Department of Physics, Purdue University, West Lafayette, Indiana 47907*

(Received 1 July 1985)

We report the first well-resolved, sharp-line electronic Raman (ER) spectra of shallow acceptors in GaAs. The material-dependent circumstances of these observations are particularly interesting. The spectra, taken with cw, neodymium-doped yttrium-aluminum-garnet (Nd:YAG) laser radiation at  $\sim 15$  K, were observed only in undoped, semi-insulating bulk GaAs, grown by the liquid-encapsulated Czochralski technique. The residual, shallow acceptors present in such material are completely compensated by the double donor, mid-band-gap defects EL2. The latter, in their metastable form, provide the essential means whereby a nonequilibrium population of holes can be generated and maintained on the acceptors. This situation is exploited to obtain a detailed analysis of the ER spectra of the shallow acceptors in this technologically important material, including the identification of the residual acceptors (C and Zn), the estimates of their concentration ( $\ll 10^{16}$   $\text{cm}^{-3}$ ), the testing of their adherence to the parity selection rule, and their response to internal strains and electric fields. A comparison of ER spectra is made with  $p$ -type, semiconducting bulk GaAs, where only broad, unresolved spectra are obtained, presumably because of much greater acceptor concentrations ( $> 10^{16}$   $\text{cm}^{-3}$ ).

### I. INTRODUCTION

Electronic Raman (ER) spectra<sup>1,2</sup> for bound holes on acceptors, showing their transitions from the ground to the excited states, have been reported for a number of  $p$ -type semiconductors, e.g., Si,<sup>3-6</sup> Ge,<sup>7</sup> GaP,<sup>8-10</sup> and GaAs.<sup>4,11</sup> Well-resolved spectra, with fairly narrow lines, have been obtained for all the materials except GaAs. For the latter, the spectra reported for a given impurity in doped  $p$ -type bulk crystals, consisted of a single, greatly broadened peak with no resolvable structure. In contrast, the far-infrared, thermally-assisted photoconductivity spectra obtained by Kirkman *et al.*<sup>12</sup> in high-quality, epitaxial  $p$ -type GaAs contained sharp, highly resolved structure. The extreme broadening and lack of resolution of the ER spectra in the bulk-grown samples has never been clarified. Two factors have been cited: the overlap of the extended wave functions of the excited states when the impurity concentration is large,<sup>11</sup> and phonon wings due to vibronic coupling of the impurity ground state with the host lattice, an effect which might be particularly applicable in polar or piezoelectric materials.<sup>4</sup>

In the present work, we report ER spectra for shallow acceptors in bulk GaAs which are strikingly different from those reported before. There are two aspects of our results that are particularly interesting:

(1) In measurements made with relatively weak, cw Nd:YAG (neodymium-doped yttrium-aluminum-garnet) laser radiation, we have obtained very sharp Raman spectra in bulk GaAs, comparable in linewidth and resolution to the far-infrared spectra observed<sup>12</sup> in high-quality, epitaxial material.

(2) Our ability to observe such spectra was highly dependent on the nature of the host material. Rather surprisingly, these results were obtained only in undoped, semi-insulating (SI) GaAs, grown by the liquid-

encapsulated Czochralski (LEC) technique.<sup>13</sup>

This material has attracted much attention because of its technological importance as a substrate for GaAs device fabrication, and also because of the many interesting and still puzzling aspects of the quenching phenomena<sup>14</sup> associated with metastable states of its mid-band-gap defects. In such SI material the bound-hole population which we have observed on the shallow acceptors by ER scattering must be present in a nonequilibrium state. We believe that the mid-band-gap defects EL2, particularly in their metastable state, play a critical role in facilitating the generation and maintenance of such a hole population. Thus it is particularly useful and significant that electronic Raman scattering can help to characterize this material by detecting and identifying the residual acceptors, and also by providing indirect information relating to the properties of the EL2 defects.

We shall briefly outline and explain the material-dependent aspects of our observations in Sec. III, but a more complete report and analysis will be presented elsewhere. Our main objective in this paper is to show how the unusual material circumstances can be exploited to obtain the first detailed analysis of the ER spectra of shallow acceptors in GaAs. The following features will be emphasized: (i) a comparison of the ER spectra for the shallow acceptors (C and Zn, in the present experiments) with the well-characterized, far-infrared spectra for these acceptors in deliberately doped, epitaxial material. This served to identify the unknown acceptors in the undoped, SI material, and also to illustrate the difference in the parity selection rule for the two techniques; (ii) a comparison of the sharp-line Raman spectrum in undoped, SI GaAs with the very broad spectrum for the same acceptor in the doped  $p$ -type material; (iii) an analysis of the dependence of the spectra on scattering configuration and polarization; (iv) a survey of some sample-dependent aspects of

TABLE I. Specifications of undoped, LEC-grown SI GaAs samples. In the remarks,  $x$  is the arsenic atom fraction in melt during the growth of the material; SSMS represents spark source mass spectroscopy.

Sample designation <sup>a</sup>	Supplier	Dimensions (mm×mm×mm)	Sample orientation	Supplier's remarks	Acceptor observed by Raman scattering
R-29F		3.0×7.0×0.5	(110),(110),(100)	EL2 $\approx$ 1.2×10 <sup>16</sup> cm <sup>-3</sup> C $\approx$ 8.0×10 <sup>15</sup> cm <sup>-3</sup> x=0.50	C
GTE	E. Johnson	3.0×2.5×2.0	(110),(110),(100)	$\rho\approx$ 10 <sup>8</sup> Ω cm	C
GY252	P. W. Yu	1.5×4.0×4.0	(110),(110),(100)	"High" C concentration	C
YU2	P. W. Yu	7.0×7.0×3.0	(110),(110),(100)	EL2 $\approx$ 10 <sup>16</sup> cm <sup>-3</sup> SSMS shows Si	Zn

<sup>a</sup>R-29F and GY252 are notations used by the suppliers of these two samples. The GTE sample was obtained from GTE Laboratories and the YU2 sample was obtained from Phil Yu.

the spectra, and their significance; (v) the effects of uniaxial stress in clarifying the Rayleigh wing.

## II. EXPERIMENTAL CONDITIONS

The ER scattering measurements were made with cw Nd:YAG laser radiation. The incident power was  $\sim$ 0.5 W, focused to a 150- $\mu$ m-diam beam in the sample. Since the absorption of such radiation is very weak ( $\sim$  a few cm<sup>-1</sup>) for GaAs, the measurements could be made in transmission, using the 90° scattering configuration. The scattered light was analyzed by a Spex double-grating monochromator, generally with 1-mm slits, giving a resolution of 4 cm<sup>-1</sup>, with measurements made at 2-cm<sup>-1</sup> intervals, except when higher resolution was desired in order to determine the natural linewidth. The detector was a RCA photomultiplier with S1 response. Its response was recorded by photon counting, generally for intervals of approximately 50 s at each wave-number setting. The data were stored in a computer, where they were corrected for grating and photomultiplier response, and binomially averaged.

Comparison of spectra for different scattering configurations and for different samples were made by normalizing the spectra either to the area of the TO-phonon line where possible, or else to the incident-laser intensity. The measurements reported here were made at  $\sim$ 15 K, with the GaAs sample mounted on the cold finger of a closed-cycle cryogenic refrigerator. At this temperature the hole population is bound completely in the ground state of the acceptors.

The SI GaAs samples were obtained from a variety of sources, as indicated in Table I. The samples were cut, polished, and oriented by x rays to provide known scattering configurations. The details of the latter, along with other properties of the samples provided by the supplier, are specified in the table.

## III. ANALYSIS OF THE MATERIAL DEPENDENCE OF THE SPECTRA

The fact that we could observe ER spectra at all in undoped, SI GaAs is intriguing. The acceptors present in such material must be residual, minority impurities, completely compensated by a smaller concentration of shallow

donors and a larger concentration of mid-band-gap, double-donor defects (EL2). The latter presumably determine the semi-insulating character of this material.<sup>15</sup> The shallow acceptors can therefore contain no holes in thermal equilibrium. The fact that we do, nevertheless, obtain Raman spectra for bound holes, indicates that a nonequilibrium population must be generated at low temperatures by the cw Nd:YAG laser radiation. Since such radiation is too weak for nonlinear, band-to-band intrinsic generation of electron-hole pairs, the excitation must be extrinsic. We believe that the mid-band-gap, EL2 defects play an important role in this process. Those defects which have lost electrons in compensating the acceptors can serve as traps for electrons which are excited by the laser from the valence band. The holes left behind in the valence band become bound to the residual acceptors at low temperature. We find that the bound-hole population is easily saturated at the (10<sup>14</sup>–10<sup>15</sup>) cm<sup>-3</sup> concentration level, even for weak incident radiation. This implies that the nonequilibrium populations of trapped electrons and bound holes cannot communicate, and hence that their lifetimes must be very long. This picture is consistent with the well-known transformation of EL2 defects, in the presence of Nd:YAG laser radiation, from a "normal" to a "metastable" state,<sup>14</sup> in which the electrons cannot communicate thermally or optically with the rest of the system. The net concentration of acceptors which can bind holes in this process must be equal to the excess concentration of shallow acceptors above that of the compensating shallow donors.

It is interesting that under similar conditions we could not observe the ER spectra for compensated shallow acceptors in Cr-doped SI GaAs, nor in  $n$ -type semiconducting material. The absence of an easily generated ER spectrum means that a large nonequilibrium hole population cannot be built up in these materials. Either the extrinsic generation mechanism involving the EL2 defects does not function here, or the nonequilibrium holes that can be generated undergo too rapid a decay.

We will present elsewhere a more detailed report of the various processes discussed above, emphasizing the role of the metastable states of the mid-band-gap defects and how they can be probed indirectly through the behavior of the

bound holes as seen in the ER spectra of the shallow acceptors.

#### IV. THE ER SPECTRA

##### A. Structure of the spectra and identification of the acceptors

In Figs. 1(a) and (b) we present examples of the sharp-line ER spectra obtained for C and Zn acceptors, in two different samples, GTE and YU2, of LEC-grown, SI GaAs. The two spectra are very similar in structure. Each contains four well-resolved peaks labeled *G*, *E*, *D*, and *C*. In Fig. 2 we specify the symmetries of the states, and relate the spectral lines to transitions between the ground state and the  $2S$  and  $2P$  excited states, following the analysis presented in the earlier spectroscopic work.<sup>12</sup> The relative shift of the spectra for the two impurities is due to core effects which give different central-cell corrections for C and Zn. As is evident from the signal-to-noise ratios of the two spectra, the net concentration of C is much greater than that of Zn. (The estimates of the actual concentrations will be presented later.) In the weaker Zn spectrum, there is additional structure, not all of which is noise; part of it is from the underlying two-phonon spectrum, e.g., the 2TA peak at  $162\text{ cm}^{-1}$ .

The identification of the acceptors is made by comparing our ER scattering data with the far-infrared spectral data<sup>12</sup> of lightly doped, *p*-type epitaxial GaAs samples. Table II shows a comparison of the energy shifts obtained for the various lines of the C and Zn spectra, as determined by the two techniques. It also gives the theoretical values for the shifts, based on the work of Lipari and Baldeschi,<sup>16</sup> as modified by estimated central-cell corrections for the two impurities.<sup>17,18</sup> The spectral data for the two experimental techniques are in excellent agreement, within  $<3\text{ cm}^{-1}$ . We refer to the earlier literature<sup>12</sup> for further discussion of the theory and the details of the

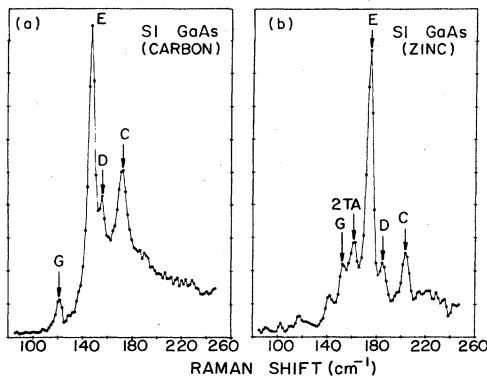


FIG. 1. ER spectra for (a) carbon and (b) zinc acceptors in GaAs. (a) and (b) are obtained for sample GTE for  $T_2$  symmetry and sample YU2 for  $E$  symmetry, respectively. The actual amplitude of the carbon spectrum is about 10 times that of the zinc spectrum. The peak, labeled 2TA, intruding in the weaker zinc spectrum, is from the background two-phonon spectrum of GaAs.

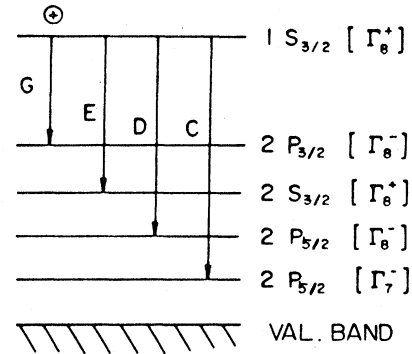


FIG. 2. Schematic diagram identifying the transitions from the ground state to various excited states in shallow acceptors. The wave functions, symmetries, and parities of the states are also specified, in accordance with Ref. 12.

spectra, since the Raman data provide no new information in this respect, except to give the values of the  $1S$  to  $2S$  transitions, which are the strongest lines in the Raman spectra and are obviously missing in the far-infrared spectra.

We emphasize here the sharpness of the Raman lines. To measure the linewidths, it was necessary to use narrower slit widths (0.25 mm with  $1\text{-cm}^{-1}$  resolution), and to take data at  $1\text{-cm}^{-1}$  intervals without smoothing. The linewidths are appreciably narrowed, approaching  $3\text{ cm}^{-1}$  for the dominant *E* line at half maximum. This is smaller than the linewidths reported for any of the other group IV or III-V materials, and is indicative of the relatively greater purity of the SI GaAs samples. Our linewidths are nearly comparable to those observed in the far-infrared spectra of the epitaxial *p*-type GaAs samples. The smallest linewidths reported in the latter case are  $\sim 1\text{ cm}^{-1}$ , for the purest samples.

The profound differences in the relative intensities of the various lines in the Raman and far-infrared spectra re-

TABLE II. Identification of acceptors and their Raman transitions. All values for shifts are expressed in  $\text{cm}^{-1}$ .

Line <sup>a</sup>	Symmetry	Theory <sup>b</sup>	Far-infrared spectroscopy <sup>c</sup>	Raman scattering
Carbon				
<i>G</i>	$A_1 + E + T_2$	118	123	122
<i>E</i>	$A_1 + E + T_2$	148		148
<i>D</i>	$A_1 + E + T_2$	152	156	155
<i>C</i>	$E + T_2$	167	172	172
Zinc				
<i>G</i>	$A_1 + E + T_2$	156	156	153
<i>E</i>	$A_1 + E + T_2$	186		174
<i>D</i>	$A_1 + E + T_2$	190	187	184
<i>C</i>	$E + T_2$	205	202	203

<sup>a</sup>The relevant transitions are shown in Fig. 2.

<sup>b</sup>The theoretical values are taken from Table I of Ref. 17.

<sup>c</sup>Reference 12.

flect the complementarity of the parity selection rule which governs the two processes, the one-photon far-infrared absorption process and the two-photon Raman scattering process. We have already noted that the *E* line (corresponding to the  $1S_{3/2}$ -to- $2S_{3/2}$  transition) is the strongest electronic Raman line; but is completely missing in the far-infrared spectra. Since the transition is between states of the same parity, it is allowed in Raman scattering but forbidden in absorption. On the other hand, the *G*, *D*, and *C* lines, which are allowed, and hence strong in the latter, are relatively weak in the ER spectra. If the parity selection rule for ER scattering were fully applicable for GaAs, the *G*, *D*, and *C* lines would be completely missing. This selection rule is not strictly applicable because of the lack of inversion symmetry. However, for the higher excited states with their larger orbits, the lack of inversion symmetry is less significant. The *C* line should be most affected and hence be the weakest line in this group, but actually it is the strongest. This may be attributed to the presence of internal electric fields, e.g., from ionized impurities. Electric fields mix *S* and *P* wave functions<sup>19,17</sup> and thus permit the parity-forbidden processes to be bypassed; the larger the orbit, the more effectively can the selection rule be violated. To the extent that the internal fields vary from sample to sample, we can expect the relative intensity of the *C* line in a spectrum to be sample dependent. This aspect will be examined further in Sec. IV E.

The excitation energies of carbon and zinc acceptors in GaAs have also been observed by photoluminescence<sup>18</sup> and selective-excitation-luminescence<sup>17</sup> measurements. In the former, the energies of the various *S* states can be obtained. In the latter, the transitions from the ground state to the  $2S$  and  $2P$  states have been observed. A comparison of these results with those of the far-infrared photoconductivity was presented by Hunter and McGill.<sup>17</sup> The disadvantage of this technique is that the transition lines are relatively broad and can be obscured by a strong luminescence background.

#### B. Comparison with ER spectra for *p*-type semiconducting GaAs

It is interesting to compare a sharp-line spectrum obtained in an undoped, SI GaAs sample (YU2) with the highly broadened spectrum observed in a *p*-type semiconducting GaAs sample. In Fig. 3 we present such a contrast for the case of Zn acceptors. The sharp-line spectrum is much weaker and is shown here expanded by a factor of 25 (after normalization by the TO lines). For the *p*-type sample the peak of its spectrum coincides with the position of the dominant *E* line at  $174\text{ cm}^{-1}$ , and there is a hint of the *G* line, which shows up as a shoulder. Otherwise, the structure is completely washed out.

The contrast between the two spectra cannot be attributed to a phonon wing; if such a wing existed one would expect it to occur in all GaAs samples. Rather, we believe that the broadening of the lines and loss of resolution in the *p*-type sample is due to its much greater concentration of acceptors, and the consequent overlap of the wave functions, especially in the excited states.

To make our analysis more quantitative, we can estimate the relative acceptor population in the two samples. From the normalized spectra of Fig. 3, we obtain a ratio of  $\sim 40$  for the heights of the peaks at the position of the *E* line; this represents a lower limit for the relative concentration of acceptors in the two samples. If, instead, we compare areas of the two spectra (to take into account broadening of the lines), we obtain an upper limit for the ratio of  $\sim 100$ . Hall measurements provided for the *p*-type sample specify an acceptor concentration of  $\sim 3 \times 10^{16}\text{ cm}^{-3}$ . Hence, the net acceptor concentration in the SI sample can be estimated to be between  $3 \times 10^{14}$  and  $8 \times 10^{14}\text{ cm}^{-3}$ . The spectrum shown in Fig. 1(a) for *C* is about 10 times stronger than the one for Zn in 1(b), but is equally sharp. Hence we conclude that sharp-line spectra are still possible for acceptor concentrations between  $3 \times 10^{15}$  and  $8 \times 10^{15}\text{ cm}^{-3}$ , and that broadening of the spectra due to merging of the spectral lines sets in rapidly when the concentration becomes a few times higher, in the  $10^{16}\text{-cm}^{-3}$  range.

For comparison, we refer to the ER spectra measured by Doehler<sup>20</sup> for Ga-doped, *p*-type Ge, where only the *E* and *C* lines could be observed. They are well resolved, half-widths of  $\sim 7\text{ cm}^{-1}$ , at an acceptor concentration of  $4.5 \times 10^{15}\text{ cm}^{-3}$ . The lines merge to a single broad peak

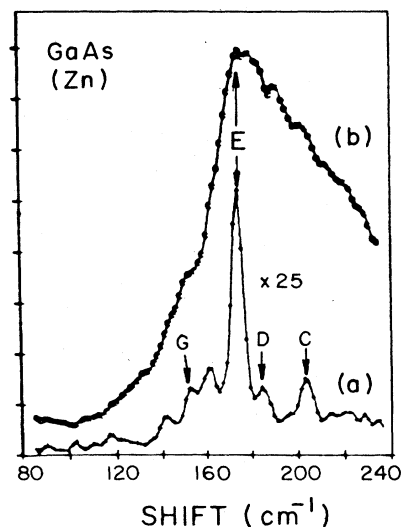


FIG. 3. Comparison of (a) the weak but sharp ER spectrum for zinc in SI GaAs with (b) the strong, broad spectrum from Zn-doped, *p*-type, semiconducting material. The sharp spectrum is shown expanded 25 times. Note that the broad spectrum peaks at the frequency shift of the *E* line and has a shoulder at the position of the *G* line. For cw Nd:YAG laser measurements, the Raman spectrum for the *p*-type semiconducting sample appears only on top of a strong luminescent background. We could suppress this background by making measurements with high-repetition-rate ( $\sim 15000\text{ Hz}$ ) *Q*-switched laser pulses ( $\sim 300\text{ ns}$  long), and using gating techniques in photon counting to eliminate the delayed luminescent part of the signal. The resulting Raman spectrum for this sample was independent of laser power.

at a concentration level of  $2.5 \times 10^{16} \text{ cm}^{-3}$ , and are completely washed out at  $7.5 \times 10^{16} \text{ cm}^{-3}$ . Since the energy shift for the  $E$  line of Ga in Ge is appreciably smaller than for C acceptors in GaAs ( $\sim 65$  versus  $148 \text{ cm}^{-1}$ ), we can expect the Bohr orbits to be smaller in GaAs than in Ge, and the merging of the lines and broadening of the spectrum to occur at higher impurity concentrations in GaAs.

There remains a puzzling aspect for the  $p$ -type GaAs spectrum to which we call attention in Fig. 4. Here we present the full range of the acceptor spectrum for this material. We note how far the tail of the broadening peak extends on the high-energy side, well beyond the ionization energy of the Zn acceptors (at  $240 \text{ cm}^{-1}$ ), and past the sharp TO and LO lines just below  $300 \text{ cm}^{-1}$ , into the continuum of the valence bands. The nature of this very extended tail, which was seen also in the earlier work,<sup>4,11</sup> for several different acceptors, is not understood.

### C. The $A$ line in the ER spectra: Strain splitting of the degenerate ground state

We turn to another feature of the spectrum in Fig. 4, the strong wing extending to  $\sim 80 \text{ cm}^{-1}$  from the Rayleigh line. Near zero energy shift, it has approximately the same intensity as the  $E$  line. From the form and position of this wing, it could be thought to be due either to single-particle scattering by free carriers, or to transitions of bound holes between the split ground states of the acceptors. Since the holes must be completely bound at low temperature, the latter alternative is the more reasonable

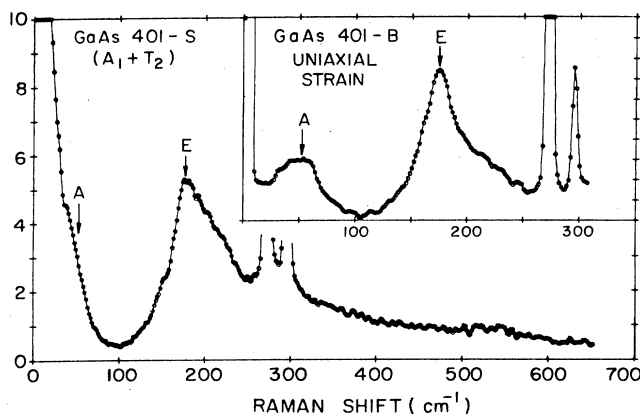


FIG. 4. The extended ER spectrum of Zn-doped  $p$ -type GaAs from sample 401-S.  $p \approx 3.0 \times 10^{16} \text{ cm}^{-3}$ . Note the broad  $A$  line near the Rayleigh line and the very extended tail. The effect of uniaxial stress is shown in the spectrum in the inset, obtained from sample 401-B in the same ingot. This sample is similar to sample 401-S, but with a slightly higher carrier concentration. Both spectra are for  $A_1 + T_2$  symmetry. The main effect of the stress on the ER spectrum for this symmetry is to displace the  $A$  line away from zero energy. The scattering configuration is  $X(Y,Y)Z$ , with  $X = \langle 110 \rangle$ ,  $Y = \langle 111 \rangle$ ,  $Z = \langle 112 \rangle$ , and uniaxial stress is along  $\langle 111 \rangle$ .

one. A rather narrow “zero-energy” wing, called the  $A$  line, was first observed by Henry *et al.*<sup>8</sup> in GaP, along with a broad phonon sideband. They attributed the  $A$  line to the inhomogeneous splitting of the fourfold-degenerate ground state by internal strains. We followed their example and applied uniaxial stress to the sample to deliberately split the ground states by a large amount. In the resulting spectrum, shown in the inset of Fig. 4, we see that the  $A$  line is now appreciably shifted away from the Rayleigh line, verifying the split-ground-state hypothesis. The detached  $A$  line is quite broad. This may be due to the inhomogeneous nature of the uniaxial strain (which was generated by a simple screw device, tightened before cooling the sample). It is not clear, however, why the original, internally strained  $A$  line is so broad. Perhaps a phonon sideband is involved here, as was suggested for GaP.<sup>8,10</sup>

The zero-energy Rayleigh wing is also present in the spectra for the undoped, SI GaAs samples, as is illustrated in Fig. 5(a). It is an expected accompaniment of the rest of the nonequilibrium, sharp-line electronic Raman spectrum. It is noteworthy that such a wing is completely absent in Cr-doped, SI GaAs, which is consistent with the absence in this material of nonequilibrium bound holes, and hence of the rest of the electronic Raman spectrum.

The uniaxial-strain test was also applied to the undoped, SI GaAs. The results shown in Figs. 5(b) and 5(c) for two increasing levels of strain (uncalibrated) are obvi-

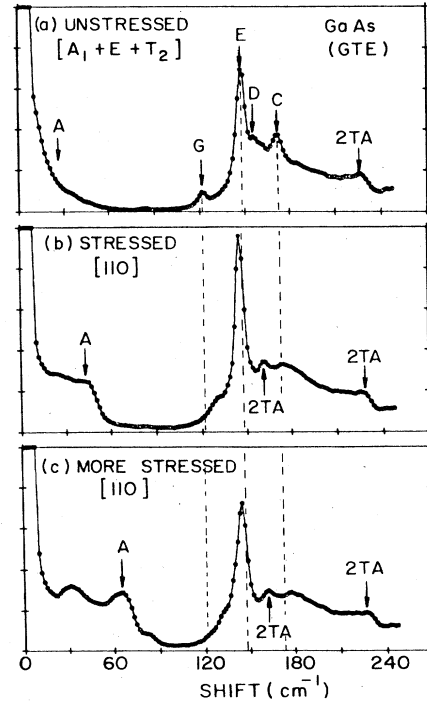


FIG. 5. Stress dependence of the ER spectrum in undoped, LEC-grown SI GaAs. The stresses labeled in these spectra are not normalized. The dotted vertical lines in (b) and (c) indicate the position of the unshifted Raman lines. The stress is along  $\langle 110 \rangle$ . The scattering configuration is  $X(Y,Y)Z$ , with  $X = \langle 110 \rangle$ ,  $Y = \langle 110 \rangle$ , and  $Z = \langle 100 \rangle$ .

ously more complicated than in the  $p$ -type sample. The Rayleigh wing is pushed out, extending to larger shifts with increasing strain, and it is much more structured. It seems to be made up of several components: there are two large peaks which respond with different sensitivity to increasing strain, and also a component which is not responsive and remains fixed near zero energy. The magnitude of the strain-induced shift of the outermost of the two large displaced peaks in the wing is comparable to that in the  $p$ -type sample. If we attribute one of these peaks to the  $A$  line of the shallow acceptors, the rest of the structure, which is not present in the  $p$ -type sample, is perhaps attributable, by default, to the population of electrons, both equilibrium and nonequilibrium, which reside in the metastable states of the mid-band-gap defects. If this supposition is correct, further studies of the Rayleigh wing with more careful uniaxial-strain measurements, to minimize inhomogeneous broadening effects and give sharper structure, may provide a new means for studying the metastable states of the EL2 defects.

There is also information in Fig. 5 on the effect of the external stress on the individual lines of the ER spectra. The  $E$  line is shifted very slightly to lower energy. The  $G$  line is shifted to higher energy, so that the  $E$  and  $G$  lines tend to merge. We lose track of the  $D$  line. At first sight it appears to be shifted up to  $162\text{ cm}^{-1}$ , but we believe that the  $162\text{-cm}^{-1}$  peak is really due to underlying  $2TA$ -phonon peaks; note that it does not continue to move with increasing strain! The  $C$  line appears diminished, broadened, and shifted to higher energy. (It shows up more clearly in another scattering configuration, in which the underlying phonon spectrum is suppressed.) Since the

energy difference between the  $1S$  and  $2S$  states is decreased, it means that the splitting of the  $2S$  state is slightly larger than that of the  $1S$  state provided there are no shifts in the "center of gravity" of the energies of the two states. With the same proviso, since the energy difference between the  $1S$  and  $2P$  states is increased, it means that the splitting of the  $2P$  states is smaller than that of the  $S$  states. The  $2P_{5/2}$  state with  $\Gamma_7$  symmetry is expected to shift but not split.<sup>21</sup> However, all these changes in the positions of the spectral lines are small compared to the splitting of the ground state, as measured by the displacement of the  $A$  peak with strain.

We also note that there is no "doubling" of spectral lines due to the splitting of the various states. Since the splitting of the  $1S_{3/2}$  state is large,  $\sim 64\text{ cm}^{-1}$  or  $\sim 8\text{ meV}$  for the larger strain, according to the displacement of the outermost peak of the  $A$  line, only the lower ground state can be occupied by holes at low temperature and only it is capable of contributing to the Raman structure. Also, it implies that we do not see any transitions between the lower of the split ground states and the higher of the split excited states.

#### D. Symmetry analysis of the ER spectra

In Fig. 6(a) we present ER spectra for four different scattering configurations (including polarization), as indicated in the figure captions. These correspond to the following symmetry designations of the spectra: (i)  $A_1 + E + T_2$ , (ii)  $E$ , (iii)  $A_1 + E$ , and (iv)  $T_2$ . The spectra have been normalized and corrected for the different response to the variation in polarization of the scattered

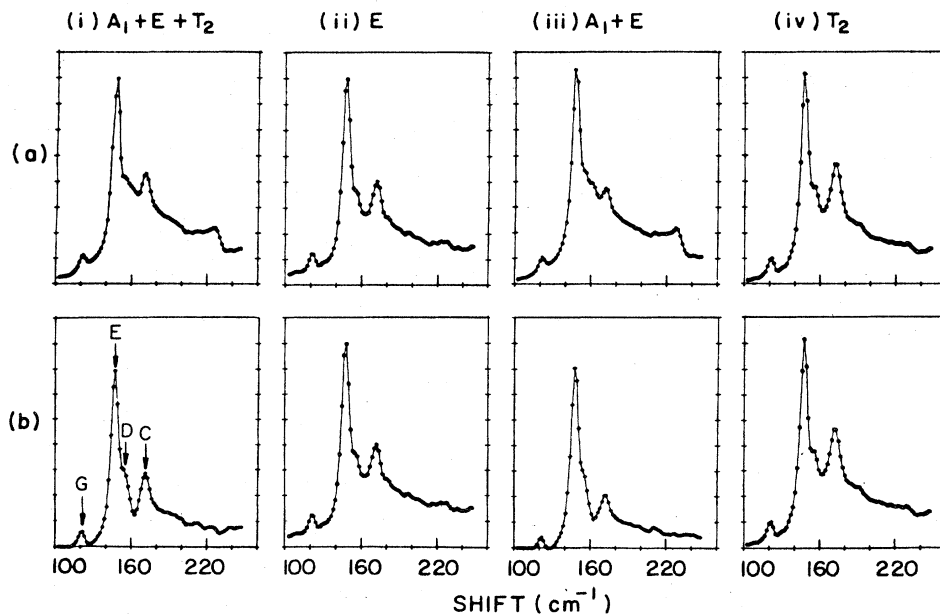


FIG. 6. (a) Symmetry dependence of the ER spectrum as measured. (b) Symmetry dependence of the ER spectrum, after subtracting the contribution of overtone phonon scattering in configurations (i) and (iii). The scattering configurations are (i)  $X(Y,Y)Z$ , (ii)  $X(Y,X)Z$ , (iii)  $X(Z,Z)Y$ , and (iv)  $X(Z,X)Y$ , with  $X$ ,  $Y$ , and  $Z$  as in Fig. 5.

light incident on the spectrometer gratings. Clearly, there is no strong dependence of the spectra on the different symmetries of the spectra. All four lines— $G$ ,  $E$ ,  $D$ , and  $C$ —appear in all cases, with nearly the same relative intensities, except for the  $C$  line. The  $C$  line seems relatively weaker in cases (i) and (iii) which was observed here with the incident and scattered light having parallel polarization. However, to some extent this is an artifact due to the underlying contribution from the two-phonon spectrum. The strongest contribution from the latter is from overtones, which appear with the greatest prominence in the spectra with the  $A_1$ -symmetry component, i.e. in cases (i) and (iii). The phonon spectra are dominated by a 2TA peak at  $162\text{ cm}^{-1}$ , which obscures a strong minimum in the ER spectrum, and another 2TA peak at  $227\text{ cm}^{-1}$ , which is visible as a step in cases (i) and (iii). We can subtract the overtone spectrum in cases (i) and (iii) by using known two-phonon spectra from samples which do not show the nonequilibrium ER spectrum. The 2TA peak at  $227\text{ cm}^{-1}$  provides a good marker for such subtraction. The corrected results are shown in Fig. 6(b). The two-phonon contributions to the spectra in the other two symmetries are smaller, but harder to subtract because no equivalent marker is available. The residual two-phonon structure probably accounts for the somewhat greater uplift of the base of the  $E$  and  $T_2$  spectra in cases (ii) and (iv), respectively. From the corrected spectra we can conclude that the  $C$  line is the one most susceptible to the differences in scattering symmetry, being strongest in the spectra that contain the  $T_2$ -symmetry component. This result is similar to the one observed by Doehler<sup>7</sup> in Ge, where the ratio of the  $C$  to  $E$  lines is also largest in the spectra with  $T_2$  symmetry.

According to the symmetries of the states of the shallow acceptors (see Table II), the  $G$ ,  $E$ , and  $D$  lines have  $A_1 + E + T_2$  symmetry, while the  $C$  line has  $E + T_2$  symmetry. Klein<sup>1</sup> has estimated that the scattering for the fully symmetric  $A_1$  component for the shallow acceptors is zero for nonzero frequency shift. Then the scattering strengths of all four lines should be determined only by the  $E$ - and  $T_2$ -symmetry components. Furthermore, since all the lines appear in nearly equal strengths in configurations with only  $E$ - or  $T_2$ -symmetry components, we can conclude that the scattering strengths for both these components are nonzero, and, in fact, quite comparable, except for the  $C$  line.

#### E. Sample-dependent features

Some sample-dependent features of ER scattering are evident from the carbon spectra shown in Fig. 7 for three different GaAs samples. The various spectra are all for  $T_2$  symmetry, and are shown normalized to their TO lines.

The variation in height of the  $E$  lines provides a measure of the variation in carbon concentration (after compensation by shallow donors). We see here a factor-of-3 variation. Earlier, we estimated the carbon concentration in Sample GY252 as  $(3.0\text{--}8.0) \times 10^{15}\text{ cm}^{-3}$ . We note that the heights of the other lines follow the variations in the  $E$  line. This is particularly noticeable for the  $G$  and  $A$

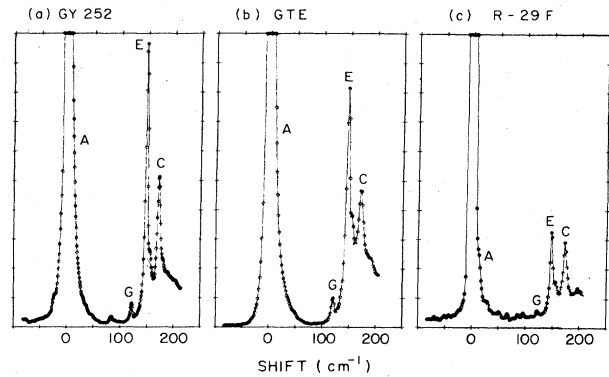


FIG. 7. Sample-dependent features of ER scattering for samples (a) GY252, (b) GTE, and (c) R-29F. All spectra are for  $T_2$  symmetry. The  $A$  lines are also shown. Three sample-dependent features are described in the text.

lines. The  $C$  line is an exception, which we consider next.

There is a variation in the ratio of the intensities of the  $C$  and  $E$  lines, from 0.4 to 0.3 to 0.7, with the exact specification made difficult by the variations in the underlying base of the spectra, due at least in part to two-phonon structure. Two reasons for the variations in the  $I_C/I_E$  intensity ratio may be cited. One is a variation in local electric fields which may influence the degree to which the parity selection rule for the  $C$  line is violated. Another possibility is a variable background presence of the impurity zinc. The  $E$  line of zinc ( $174\text{ cm}^{-1}$ ) is extremely close to the  $C$  line of carbon ( $172\text{ cm}^{-1}$ ). Because the  $E$  line is always so strong, a small amount of zinc could have an appreciable influence on the apparent magnitude of the  $C$  line of carbon.

#### V. SUMMARY AND CONCLUSIONS

In this work we have reported (i) the first observation and detailed analysis of well-resolved, sharp-line electronic Raman spectra of bound holes on shallow acceptors in GaAs, and (ii) the unusual material-dependent circumstances that these observations could be made only in undoped, LEC-grown SI GaAs, where the acceptors are a minority constituent and are compensated by double-donor, mid-band-gap defects under equilibrium conditions. The spectra are obtained for a nonequilibrium population of bound holes which is generated by the weak, cw Nd:YAG laser radiation used for the Raman scattering studies. An essential role in the generation and maintenance of the bound-hole population is played by the mid-band-gap EL2 defects, which provide metastable states in which the nonequilibrium electrons that are generated can be stored and prevented from recombining with the bound nonequilibrium holes.

We could identify the unknown carbon and zinc acceptors in our undoped semi-insulating samples from their characteristic sharp-line spectra. The earlier studies of the far-infrared spectra for shallow acceptors in deliberately doped, epitaxial GaAs provided a basis for this

identification. New information about the impurity spectra could be obtained from the different parity selection rule operating for Raman scattering, and from the observation of Raman transitions (the  $A$  line in the Rayleigh wing) between the split ground states, when the fourfold degeneracy is broken by internally and/or externally generated uniaxial strain. The sharp-line spectra also provided the first opportunity for detailed study of other characteristics of the ER spectra in bulk GaAs, such as the degree of adherence to the parity selection rule in this material, and the sample-dependent violation of the selection rule due to internal electric fields.

Our sharp-line spectra were contrasted with the extremely broad, unresolved spectra observed in  $p$ -type, semiconducting GaAs. The larger concentration of acceptors in the latter case, with its attendant overlap of wave functions for the excited states, is believed to be responsible for much of the broadening of the spectral lines and loss of spectral resolution. However, the very great extent of the tail on the high-energy side of the broad spectra peak is still a mystery.

We have demonstrated that electronic Raman scattering is a valuable tool for characterizing important features of the technologically important material, undoped, LEC-grown SI GaAs, such as the identity and relative concentrations of residual shallow acceptors, the presence of internal electric fields and strains, and, not least, the metastable states of the mysterious mid-band-gap defects EL2.

#### ACKNOWLEDGMENTS

We gratefully acknowledge discussions with E. Johnson, P. W. Yu, K. Elliott, and S. G. Bishop, which introduced us to some of the mysteries of semi-insulating GaAs and the EL2 defects. We are indebted to A. K. Ramdas and S. Rodriguez for useful and informative discussions of many of the fine points about shallow acceptors. We are also grateful to several of the above for supplying GaAs crystals which were essential for our work. This work was supported by the National Science Foundation through Grant No. DMR-82-17442.

<sup>1</sup>M. V. Klein, in *Light Scattering in Solids*, edited by M. Cardona (Springer, Heidelberg, 1975), p. 147.

<sup>2</sup>W. Hayes and R. Loudon, *Scattering of Light by Crystals* (Wiley, New York, 1978).

<sup>3</sup>G. B. Wright and A. Mooradian, *Phys. Rev. Lett.* **18**, 608 (1967).

<sup>4</sup>G. B. Wright and A. Mooradian, in *Proceedings of the 9th International Conference on the Physics of Semiconductors, Moscow, 1968* (Nauka, Leningrad, 1968), p. 1067.

<sup>5</sup>J. M. Cherlow, R. L. Aggarwal, and B. Lax, *Phys. Rev. B* **7**, 4547 (1973); **9**, 3633(E) (1974).

<sup>6</sup>Kanti Jain, Shui Lai, and Miles V. Klein, *Phys. Rev. B* **13**, 5448 (1976).

<sup>7</sup>J. Doehler, *Phys. Rev. B* **12**, 2917 (1975).

<sup>8</sup>C. H. Henry, J. J. Hopfield, and L. C. Luther, *Phys. Rev. Lett.* **17**, 1178 (1966).

<sup>9</sup>D. D. Manchon, Jr. and P. J. Dean, in *Proceedings of the 10th International Conference on the Physics of Semiconductors, Massachusetts, 1970*, edited by S. P. Keller, J. C. Hensel, and F. Stern (United States Atomic Energy Commission, Division of Technical Information, Oak Ridge, Tenn., 1970), p. 1067.

<sup>10</sup>L. L. Chase, W. Haynes, and J. F. Ryan, *J. Phys. C* **10**, 2957 (1977).

<sup>11</sup>A. Mooradian, in *Laser Handbook*, edited by F. T. Arecchi and E. O. Schulz-Dubois (North-Holland, Amsterdam, 1972), Vol. 2, p. 1409.

<sup>12</sup>R. F. Kirkman, R. A. Stradling, and P. J. Lin-Chung, *J. Phys. C* **11**, 419 (1978).

<sup>13</sup>For review of SI GaAs, see *Semiconductors and Semimetals*, edited by R. K. Willardson and A. C. Beer (Academic, New York, 1984), Vol. 20.

<sup>14</sup>See, for example, G. M. Martin, *Appl. Phys. Lett.* **39**, 748 (1981); G. Vincent, D. Bois, and A. Chantre, *J. Appl. Phys.* **53**, 3643 (1982); A. Mitonneau and A. Mircea, *Solid State Commun.* **30**, 157 (1979); Alice L. Lin, Eric Omelianovski, and Richard H. Bube, *J. Appl. Phys.* **47**, 1852 (1976); E. R. Weber, H. Ennen, U. Kaufmann, J. Windscheif, J. Schneider and T. Wosinski, *ibid.*, **53**, 6140 (1982).

<sup>15</sup>D. E. Holmes, R. T. Chen, Kenneth R. Elliott, C. G. Kirkpatrick, and Phil. Won Yu, *IEEE Trans. Microwave Theor. Tech.* **MTT-30**, 949 (1982).

<sup>16</sup>A. Baldereschi and N. O. Lipari, *Phys. Rev. B* **9**, 1525 (1974).

<sup>17</sup>A. T. Hunter and T. C. McGill, *Appl. Phys. Lett.* **40**, 169 (1982).

<sup>18</sup>D. J. Ashen, P. J. Dean, D. T. J. Hurler, J. B. Mullin, A. M. White, and P. D. Greene, *J. Phys. Chem. Solids* **36**, 1041 (1975).

<sup>19</sup>D. M. Larson, *Phys. Rev. B* **8**, 535 (1973).

<sup>20</sup>A more extensive discussion of concentration broadening is given by Doehler, in Ref. 7, for Raman spectra of Ge. See also C. Jagannath, Z. W. Grabowski, and A. K. Ramdas [*Phys. Rev. B* **23**, 2082 (1981)] for concentration broadening in Si.

<sup>21</sup>S. Rodriguez, P. Fisher, and F. Barra, *Phys. Rev. B* **5**, 2219 (1972).